MDPI

Article

Comparison of Rainfall-Runoff Simulation between Support Vector Regression and HEC-HMS for a Rural Watershed in Taiwan

Shen Chiang, Chih-Hsin Chang and Wei-Bo Chen *

National Science and Technology Center for Disaster Reduction, New Taipei City 23143, Taiwan; johnson@ncdr.nat.gov.tw (S.C.); chang.c.h@ncdr.nat.gov.tw (C.-H.C.)
* Correspondence: wbchen@ncdr.nat.gov.tw; Tel.: +886-2-81958621

Abstract: To better understand the effect and constraint of different data lengths on the data-driven model training for the rainfall-runoff simulation, the support vector regression (SVR) approach was applied to the data-driven model as the core algorithm in the present study. Various features selection strategies and different data lengths were employed in the training phase of the model. The validated results of the SVR were compared with the rainfall-runoff simulation derived from a physically based hydrologic model, the Hydrologic Modeling System (HEC-HMS). The HEC-HMS was considered a conventional approach and was also calibrated with a dataset period identical to the SVR. Our results showed that the SVR and HEC-HMS models could be adopted for short and long periods of rainfall-runoff simulation. However, the SVR model estimated the rainfall-runoff relationship reasonably well even if the observational data of one year or one typhoon event was used. In contrast, the HEC-HMS model needed more parameter optimization and inference processes to achieve the same performance level as the SVR model. Overall, the SVR model was superior to the HEC-HMS model in the performance of the rainfall-runoff simulation.

Keywords: rainfall-runoff simulation; support vector regression; HEC-HMS; data-driven model; Taiwan

1. Introduction

The precision and robustness of rainfall-runoff simulations are essential to watershed modeling from various perspectives, such as planning and designing soil conservation practices, irrigation water management, wetland restoration, stream restoration, water-table management, and water resources planning, development, and management [1]. There are various styles of rainfall-runoff models worldwide developed to solve these issues from the manners of deterministic, probabilistic, or stochastic approaches [2]. For a well-gauged watershed, a hydrologic model with an appropriate scheme that meets the watershed characteristics can be applied for the rainfall-runoff modeling. However, for poorly gauged or ungauged watersheds, a physically based hydrologic model is preferred for reasonable parameter estimation processes [3]. For the convenience of applying hydrologic models, a software package with graphic user interface (GUI) makes the rainfall-runoff simulation task easier.

The Hydrologic Modeling System (HMS), developed by the Hydrologic Engineering Center (HEC) of the U.S. Army Corps of Engineering Center, the HEC-HMS, is one of the most popular rainfall-runoff simulation tools worldwide, including many traditional rainfall-runoff simulation tools hydrologic analysis procedures [2]. The HEC-HMS is designed to simulate the complete hydrologic processes of dendritic watershed systems in event-based simulation or continuous simulation [3–6]. Different mechanisms can be selected to perform the simulation; each selection requires a different dataset corresponding to its model setting and parameter tuning. Supplemental analysis tools are provided for

model optimization, forecasting streamflow, depth-area reduction, assessing model uncertainty, erosion and sediment transport, and water quality [2]. However, in corresponding with the scheme, complexity, and objective of the rainfall-runoff model, temporal and spatial distribution data additional to single point observation data may require more information which results in massive subsequent pre-work preparation and perspiration.

In recent years, alongside the advance of hydrology, data-driven modeling based on computational intelligence and machine-learning methodologies drew mass research interest in hydrological and hydrodynamic simulation [7–13]. The model training data length/quality, the tuning of the data-driven model parameters, and the selection strategy of the feature values are particularly relevant to this kind of research in terms of credibility [14,15]. Barbero et al. [16] addressed the determination of the areal reduction factor (ARF) as a function of area and duration and demonstrated that both adequately long series and good gauge distribution are necessary for a proper investigation of the ARF.

Among the options, the support vector machine (SVM) method is a robust and efficient algorithm for classification (support vector classification, SVC) and regression (support vector regression, SVR) introduced by Vapnik et al. [17], and it has already been applied in the field of hydrology for a few decades and attained great research results: rainfall and runoff forecasting, streamflow and sediment yield forecasting, evaporation and evapotranspiration forecasting, lake and reservoir water level prediction, flood forecasting, drought forecasting, groundwater level prediction, soil moisture estimation, and groundwater quality assessment [18–21].

The object of this work was to clarify the effect and constraint of different data lengths on the data-driven model training for the rainfall-runoff simulation and to compare the performance between the data-driven model and the physical-based model in rainfall-runoff simulation. The study area, measurements, data-driven model, and physical-based model are described in Section 2. The results of the model validation for simulating watershed outflows and comparing the performance between the data-driven model and physical-based model in the rainfall-runoff simulation are presented in Section 3. In Section 4, a discussion on the advantages and disadvantages of the data-driven model and physical-based model in rainfall-runoff simulation and conclusions is given.

2. Materials and Methods

2.1. Study Area

A rural watershed located in the northern part of Taiwan was chosen as the study area. The area of the watershed is 52.1 km^2, the elevation of the watershed ranges from 180 to 960 m above sea level, and the average slope is 41.1%. A rainfall station and a water level-discharge gauging station are located within the watershed. The information for these two hydrological stations is described in Table 1, and the location of the study basin and gauging station is shown in Figure 1a,b. The Hen Chi water level gauging station is located close to the outlet of the watershed, with an elevation of 21.74 m; however, it is still higher than the minimum elevation of the watershed (about 20.0 m). Moreover, the Da Bao rainfall gauging station is located upstream of the watershed, at 600 m (as shown in Figure 1).

Table 1. The information of the rainfall and water level gauging station.

Station ID	Name	Elevation	TWD97M2.X	TWD97M2.Y
01A210	Da Bao	600 m	292,574.12	2,753,355.88
1140H049	Hen Chi	21.740 m	289,877.43	2,758,720.00

Note: The coordinate system is TWD97M2.
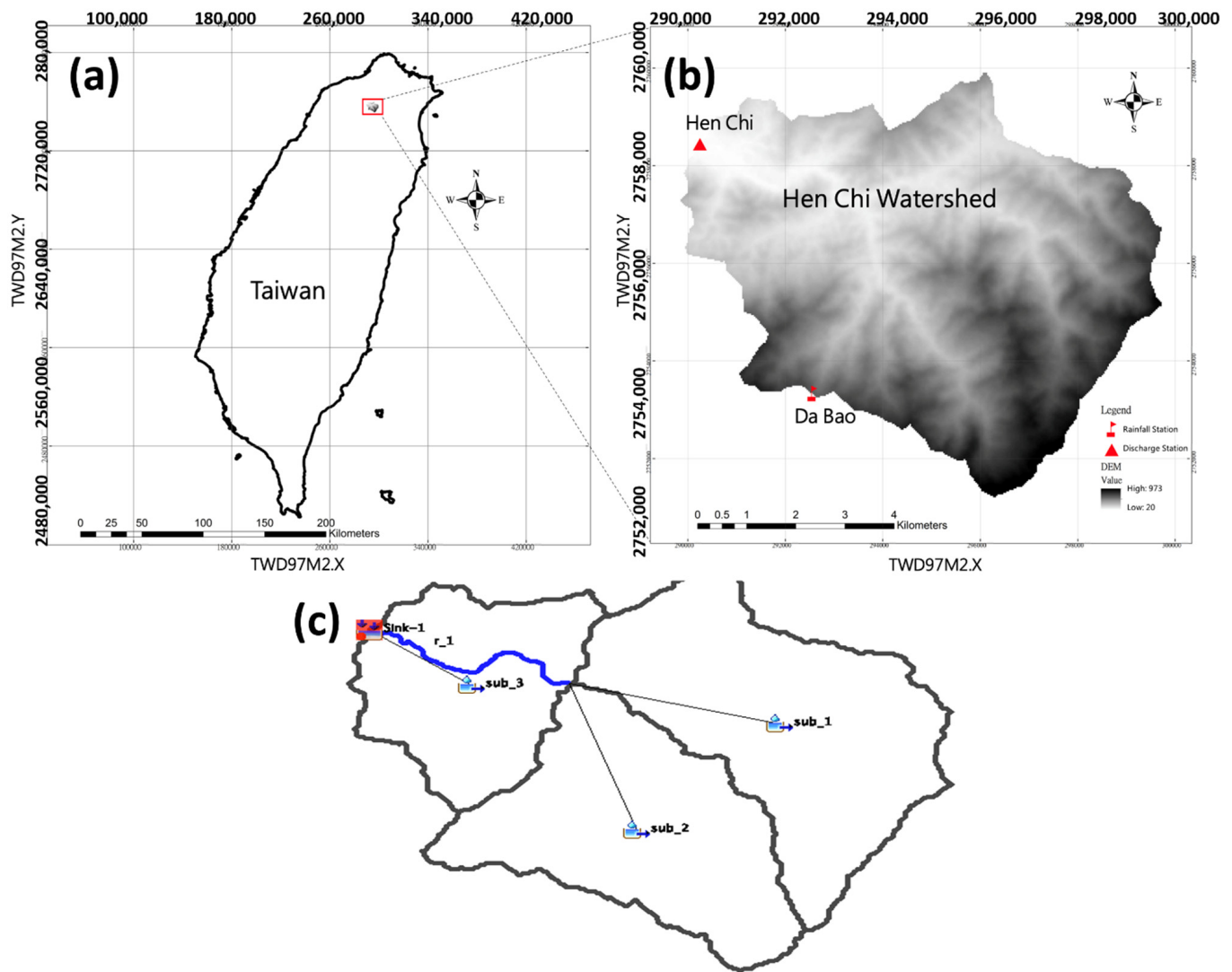
Figure 1. (**a**) the location of the studied watershed in Taiwan, (**b**) the elevations of the studied watershed, and the position of the rainfall and water level gauging stations, and (**c**) the distributions of elements divided in the HEC-HMS model for the studied watershed (Hen Chi watershed).

2.2. The Hydrologic Modeling System (HEC-HMS)

The HEC-HMS is being developed and maintained by the Hydrologic Engineering Center of the U.S. Army Corps of Engineering Center. In order to simulate the rainfall-runoff mechanism of a basin, several models needed to be established before running the HEC-HMS: the basin model, meteorologic model, control specification, time-series data, and terrain data.

2.2.1. Basin Model

A basin model consists of the elements that reflect the rainfall loss, rainfall-runoff transformation, and baseflow effect. The geographical parameters such as area, flow length, and slope of the sub-basin or reach can be automatically retrieved by the GIS module of the HEC-HMS within a DEM of the basin as an input. The basin can be divided into several sub-basins, the mainstream, and branches according to the user's interest or specific consideration. In this study, a large basin was divided into three sub-basins and one reach, with one sink outlet of the basin (as shown in Figure 1c). As for the speculation of the rainfall loss, the Soil Conservation Service (SCS) curve number (CN) loss method [22] was applied, for which the soil data and land use data were required. In this study, the land-use

data was acquired from the Ministry of Interior, and the soil-type data was acquired from the Council of Agriculture of the Executive Yuan. The mentioned data can be obtained from Taiwan Government Open Data [23]. The percentage of each land-use category and soil type are listed in Tables 2 and 3. Due to the unknown soil type being a relatively lower percentage than the others, it was considered loam in the present study. For transforming the rainfall excess, which was derived after the rainfall loss calculation, into direct runoff of the sub-basin, the Clark unit hydrograph [24] was manipulated. The time of concentration and storage coefficient needed to be determined because the relationship between these two parameters was hypothesized. There are various ways to calculate the parameters [25–29], yet the calculation results in a big range. Therefore, in this study, the two parameters were determined via the optimization module of the HEC-HMS. The Muskingum–Cunge routing method was applied for the reach flow calculation. Additionally, the recession constant and ratio to the peak were the parameters that needed to be calibrated.

Table 2. The percentage of each land-use category of the Hen Chi basin.

Land-Use Category	Percentage %
Agricultural land	25.16
Forests	69.17
Land for transportation	0.81
Water Conservancy-Use Land	0.64
Built-up land	2.50
Public facilities usage land	0.11
Recreational usage land	0.07
Mineral usage land	1.54

Table 3. The percentage of each soil type of the Hen Chi basin.

Soil Type	Percentage %
Unknown	4.53
Sandy Loam	16.56
Loam	69.25
Clay Loam, Silty Clay Loam	9.66

2.2.2. Time-Series Data and Meteorologic Model

The HEC-HMS is capable of simulating both event-based and continuous scenarios. However, for continuous simulation, the discharge peak of each rainfall event is challenging to catch through the calibration process. For this reason, after examining the data coherence and quality, 13 typhoon events were selected for the HEC-HMS parameters optimization. The selected typhoon events are listed in Table 4. The durations (hours) in Tables 4 and 5 refer to both the rainfall and runoff period. In order to make a comparison with data-driven model training, model parameters calibrated from different numbers of typhoon events are manipulated for model validation; for this purpose, two typhoon events were selected, and their information can be found in Table 5.

Table 4. Typhoon events manipulated for the HEC-HMS parameter calibration.

Typhoon Number	Typhoon Name	Max Rainfall (mm/h)	Total Rainfall (mm)	Max Discharge (cm)	Duration (h)
199111	ELLIE	46	210	126	47
199216	POLLY	21	503	149	165
199416	GLADYS	98	398	154	119
199608	HERB	31	486	243	155
199714	WINNIE	22	248	195	132
199810	ZEB	36	476	174	159
200020	XANGSANE	33	539	317	119
200407	MINDULLE	30	249	232.33	185
200420	HAIMA	37	497	245.86	104
200715	KROSA	33	551	217.91	149
200813	SINLAKU	47	725	284.59	197
200815	JANGMI	55	548	250.63	143
200908	MORAKOT	46	374	65.92	176

Table 5. Typhoon events for the HEC-HMS model validation.

Typhoon Number	Typhoon Name	Max Rainfall (mm/h)	Total Rainfall (mm)	Max Discharge (cm)	Duration (h)
201209	SAOLA	73	746	955.28	161
201513	SOUDELOR	59	574	804.27	140

2.2.3. Model Parameters Optimization

The GIS module acquires the geographical parameters in the HEC-HMS during the processing of the digital elevation data of the basin and the related field survey data.

The calibrated parameters are acquired from the built-in function named optimization trial manager of the HEC-HMS. The parameters can be retrieved via one of the criteria listed: peak-weighted RMS error, percent error peak, percent error volume, sum absolute residuals, sum squared residuals, and time-weighted error. The parameters for calibration are listed in Table 6, while the range of the parameters used the system defaults.

Table 6. The parameters for the HEC-HMS model calibration.

Element	Parameter for Optimization
r_1	Muskingum–Cunge—Manning's n—
sub_1	SCS Curve Number—Initial Abstraction
sub_2	SCS Curve Number—Initial Abstraction
sub_3	SCS Curve Number—Initial Abstraction
sub_1	Clark Unit Hydrograph—Storage Coefficient
sub_2	Clark Unit Hydrograph—Storage Coefficient
sub_3	Clark Unit Hydrograph—Storage Coefficient
sub_1	Clark Unit Hydrograph—Time of Concentration
sub_2	Clark Unit Hydrograph—Time of Concentration
sub_3	Clark Unit Hydrograph—Time of Concentration
sub_1	Recession—Ratio to Peak
sub_2	Recession—Ratio to Peak
sub_3	Recession—Ratio to Peak
sub_1	Recession—Recession Constant
sub_2	Recession—Recession Constant
sub_3	Recession—Recession Constant
sub_1	Recession—Initial Discharge
sub_2	Recession—Initial Discharge
sub_3	Recession—Initial Discharge

In hydrologic modeling, the model parameters can be inferred by estimating the distribution function of the samples [30]. In this study, the max rainfall intensity, total rainfall depth, and rainfall duration of the corresponding typhoon event were applied as the feature values of the SVR model to infer the HEC-HMS model parameter values. After the optimization process for each typhoon event, two methods of estimating the model parameters were used in this study. Type 1 used the SVR model to estimate the parameter set by using the optimized parameter values and their corresponding maximum rainfall, total rainfall, and rainfall duration as feature values to retrieve the value of each parameter. Type 2 simply used the average values of the optimized parameters.

2.3. Support Vector Regression

SVR is a variation of SVMs. SVMs are developed based on statistical learning theory [31]. The original SVMs were for solving the classification problem. The classification problem can be simplified by manipulating a kernel function by mapping the original datasets from the input space to a higher dimensional feature space. The standard support vector regression can be formed by introducing a loss function that describes the deviation of the SVMs' estimation function into the original SVMs. In brief, the basic idea of SVR is to find a model function f(x) to represent the relationship between the features and the target [32].

LIBSVM [33] is an integrated software for support vector classification (SVC), SVR, and distribution estimation. LIBSVM is an open-source package and was employed in this study for its robust and worldwide usage [34,35]. Several types of the SVMs can be selected in LIBSVM, nu-SVR; the linear kernel was applied in this study, and the default model parameter values were used. For the SVR model training, two approaches were applied. One used the typhoon events discrete data as the input, as in the HEC-HMS approach; another used continuous hourly rainfall and discharge data from 1991 to 2009, as shown in Figure 2. The datasets with the duration of 19 years (from 1991 to 2009), five years (from 2005 to 2009), two years (from 2008 to 2009), and one year (2009) were applied to acquire the SVR training model parameters.
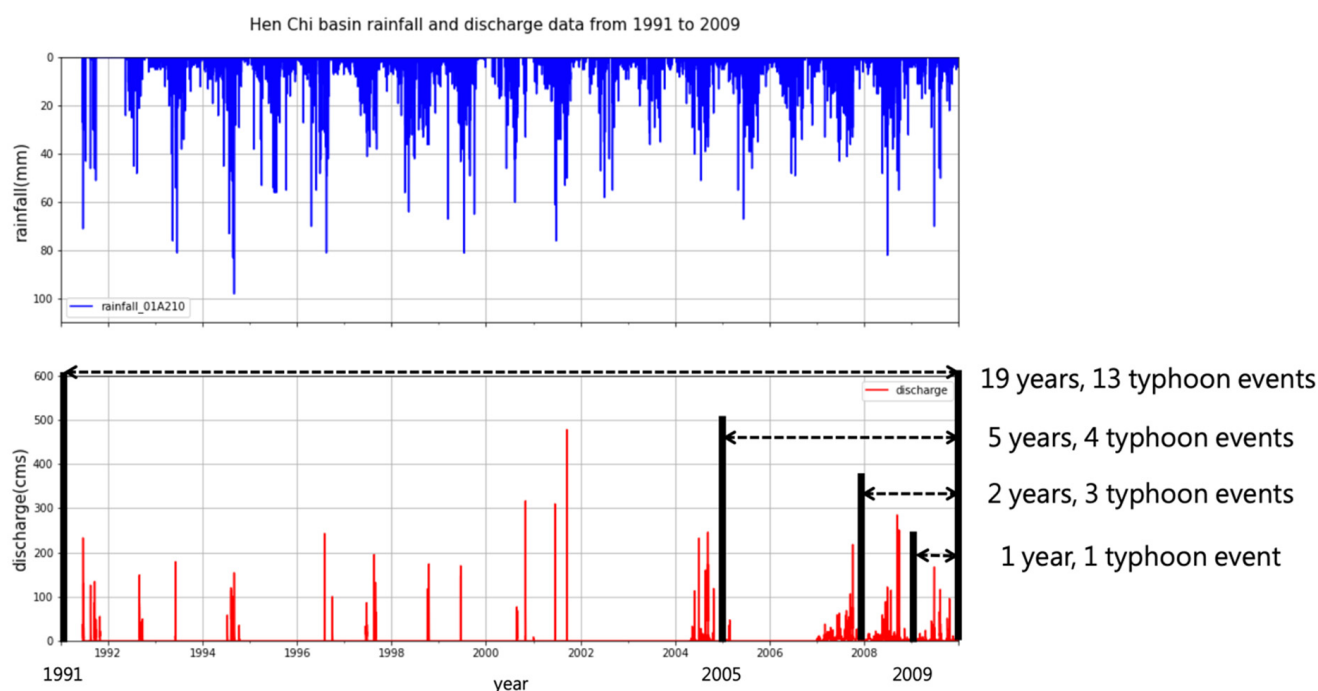
Figure 2. The time-series rainfall and discharge measurements from 1991 to 2009 for the Hen Chi watershed.

In the present study, the model target was river discharge at a specific time; the features were rainfall and discharge prior to the specific time as shown in Equation (1):

$$Dt = f(D(t - x), \dots , R(t - y), \dots), \tag{1}$$

where D denotes the discharge at time t, R denotes the rainfall, x and y are timesteps before the specific time t, where x is in the range of 1 to 3, and y is in the range 1 to 6. For instance, the feature selection of two discharge values and three rainfall values prior to the specific time t as in Equation (2):

$$Dt = f(D(t - 1), D(t - 2), R(t - 1), R(t - 2), R(t - 3)), \tag{2}$$

In the present study, SVR was applied for the data-driven model training and testing and for the inference of the HEC-HMS model parameters, as mentioned in the previous section. Two types of the model training process proceeded in this study by manipulating 19-, 5-, 2-, and 1-year ranges of observation data to proceed with the model training, denoted as Type 1. The other was the HEC-HMS parameter calibration using data from 13 typhoon events, denoted as Type 2. The SVR models with different features selection within different data types were trained and tested. In order to ensure the quality of model input data, a minimum discharge of 15 CMS was set as a criterion of data selection. The results revealed that the SVR model could estimate an excellent rainfall-runoff relationship using the observational data of a shorter period, while the HEC-HMS needed further efforts.

2.4. Model Performance Criterion

In this study, the data length limitation to rainfall-runoff simulation proceeded by comparing the simulation results performed by the HEC-HMS and the SVR model. Different data length was applied to the SVR model training and the HEC-HMS parameter calibration. The Nash–Sutcliffe efficiency (*NSE*) coefficient [36] was applied for the model performance evaluation. The formula of the *NSE* coefficient can be expressed as follows:

$$NSE = 1 - \frac{\sum_{t=1}^{T} \left(Q_o^t - Q_s^t \right)^2}{\sum_{t=1}^{T} \left(Q_o^t - \overline{Q_o} \right)^2} \tag{3}$$

where $\overline{Q_o}$ is the mean of the observation discharge, Q_o^t is the observational discharge at time t, and Q_s^t denotes the simulated discharge at time t.

It can be straightforwardly derived that the range of the Nash–Sutcliffe efficiency coefficient is $-\infty$ to 1, where 1 means the simulated discharge is identical to the observation discharge. More bias between the observation and simulated discharge makes the Nash-Sutcliffe efficiency coefficient value far smaller than 1. The performance of the modeling outcomes under different watershed dataset acquiring scenarios was also compared and discussed.

3. Results
3.1. The HEC-HMS Parameters Calibration and Validation Results

The discharge measurements recorded from 13 historical typhoon events were applied for the HEC-HMS model parameters calibration. The results are shown in Figure 3. Typhoons Saola (2012) and Soudelor (2015) were applied to validate the inferred parameter sets, as shown in Figures 4 and 5. Type 1 denotes the parameter sets inferred using SVR, and Type 2 denotes the parameter sets derived by simple average. For the convenience of comparison, the data periods of 19, 5, 2, and 1 year(s) denote 13, 4, 3, and 1 typhoon event(s). The results showed that the mean Nash–Sutcliffe coefficient of the optimized models was 0.904. However, in the model validation phase, the mean models' performance dropped to 0.754. Type 1 of the parameters' inference was better than Type 2 in a general manner. One interesting phenomenon that should be noted was that the HEC-HMS always underestimated the peak of observed discharge. The reason might be that the peak-weighted RMSE

was selected as an objective function of the optimization trial process of the HEC-HMS and this model tends to simulate the hydrograph shape more than the peak discharge. If the percent error in peak discharge was selected, the objective function might be different. Another possible reason was that the maximum discharge of the validation typhoon events was far more significant than the typhoon events used for model calibration.
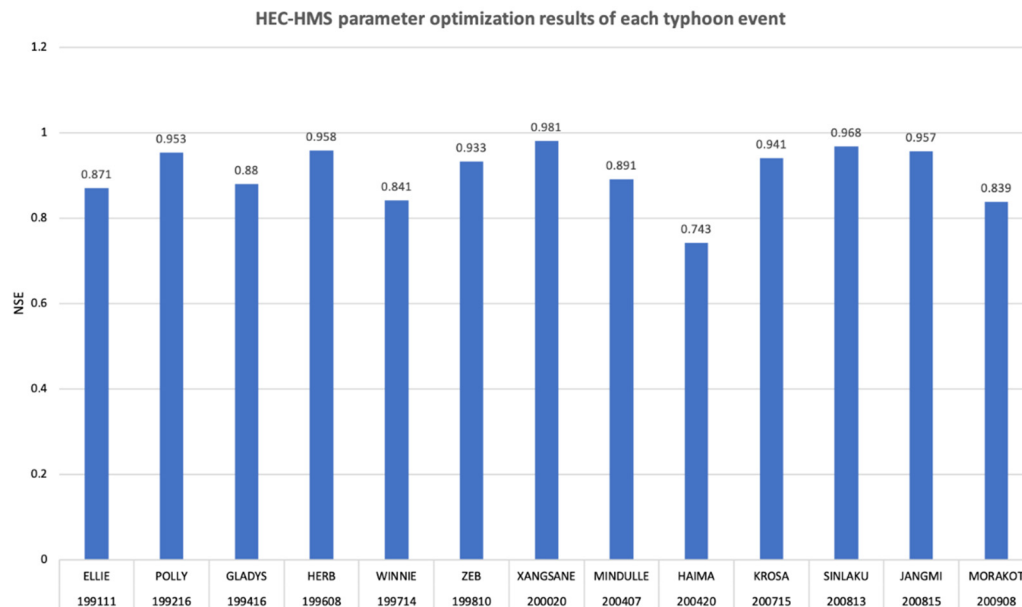
Figure 3. The *NSE* of the HEC-HMS model validation using a different parameter inference approach for each typhoon event.
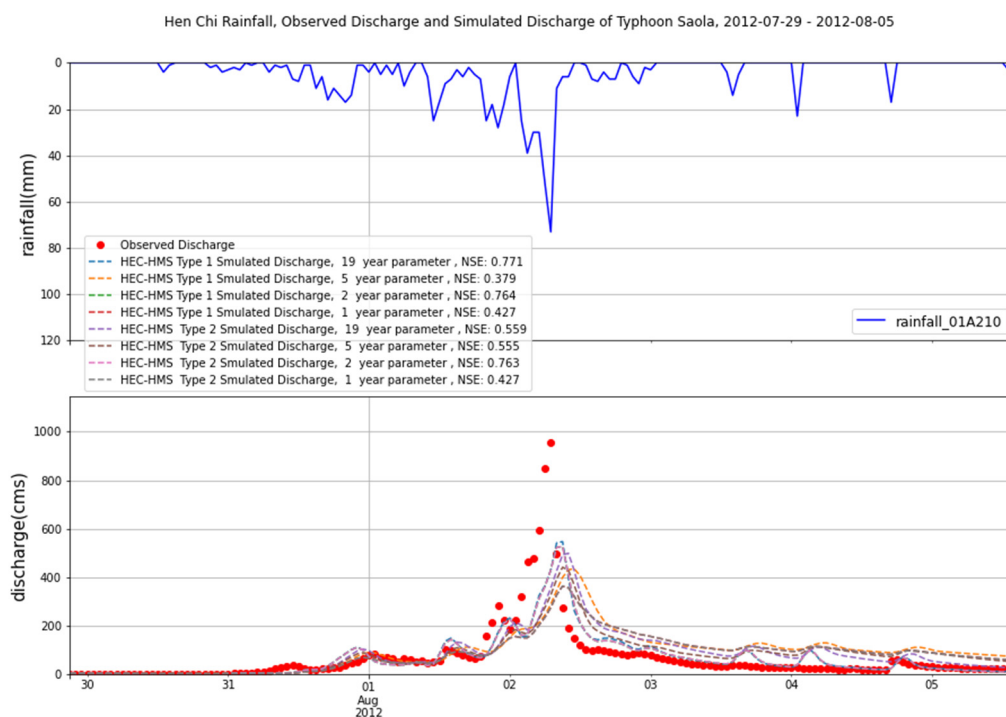
Figure 4. The measured rainfall time series (**upper** panel) and their corresponding rainfall-runoff simulations (**lower** panel) of the HEC-HMS model using different parameter optimization approaches for Typhoon Saola.
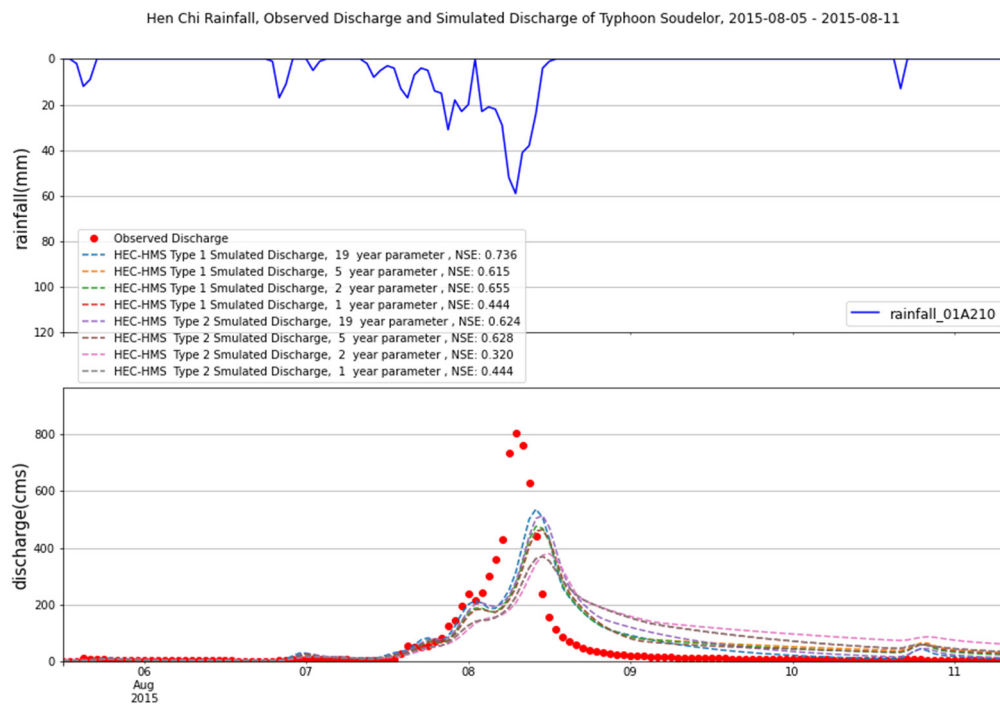
Figure 5. The measured rainfall time series (**upper** panel) and their corresponding rainfall-runoff simulations (**lower** panel) of the HEC-HMS model using different parameter optimization approaches for Typhoon Soudelor.

3.2. The SVR Model features Selection Results

Two types of the SVR model training process were conducted in the present study by manipulating 19, 5, 2, and 1 year(s) of observation data to proceed with the model training. Figures 6 and 7 show the testing results derived from the Type 1 SVR model. The other training process was the HEC-HMS parameter calibration using 13 typhoon events data (the Type 2 SVR model), as shown in Figures 8 and 9. It can be seen that the SVR model test results of Type 2 of data importing were just slightly better than Type 1.
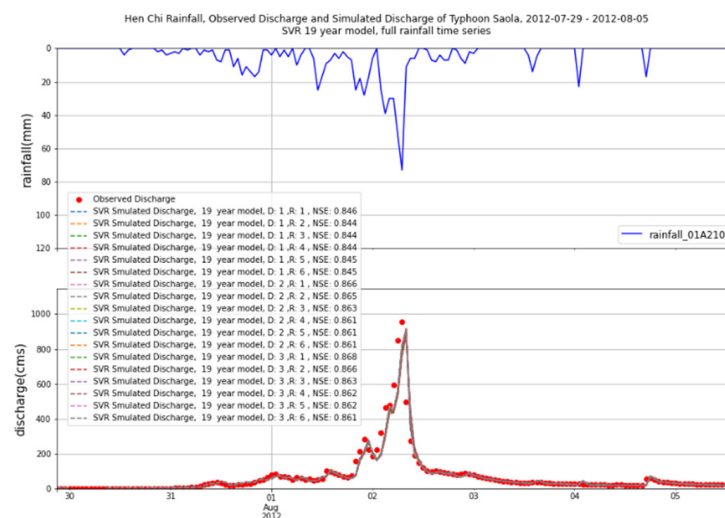
Figure 6. *Cont.*
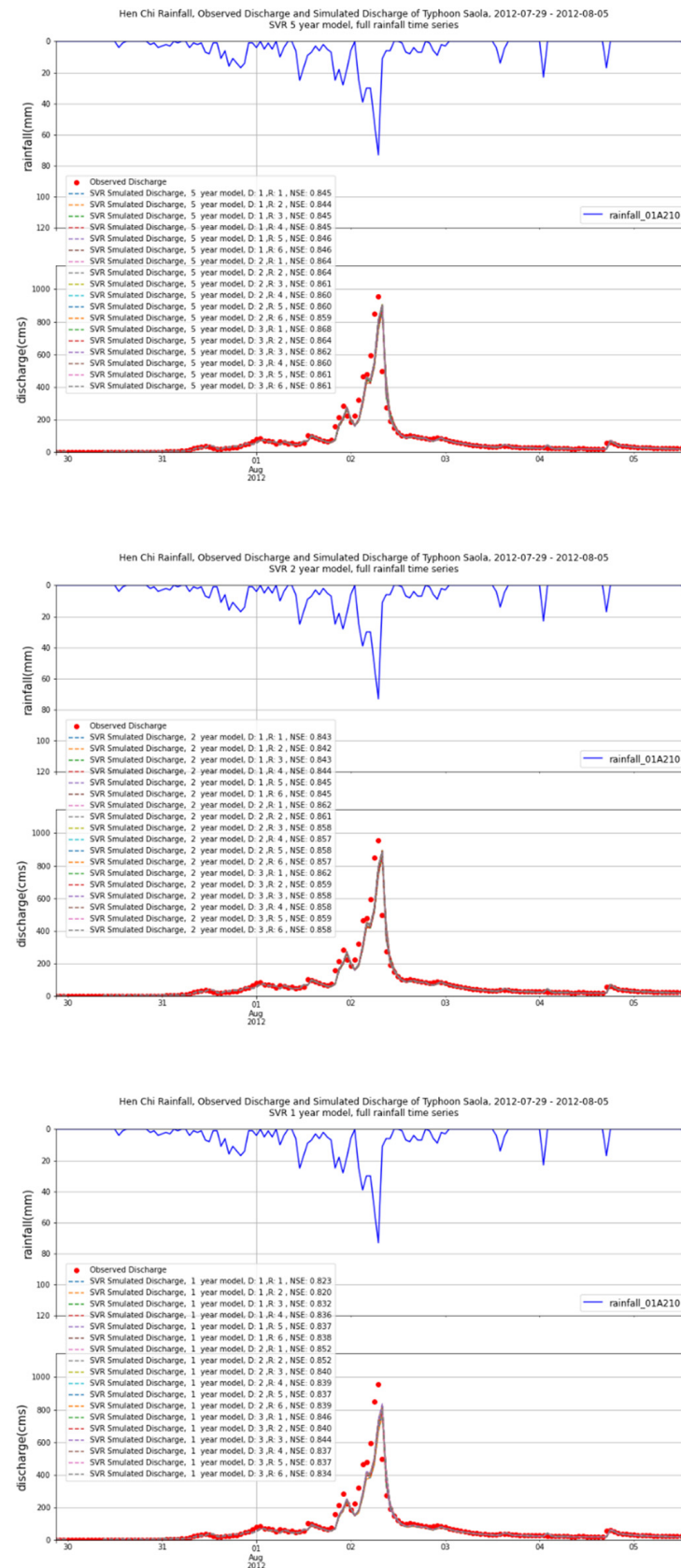
Figure 6. The testing results derived from the Type 1 SVR model using different features selection for Typhoon Saola. D 1 to 3 represents discharge features of the previous 1 to 3 h, while R 1 to 6 indicates rainfall features of the previous 1 to 6 h.
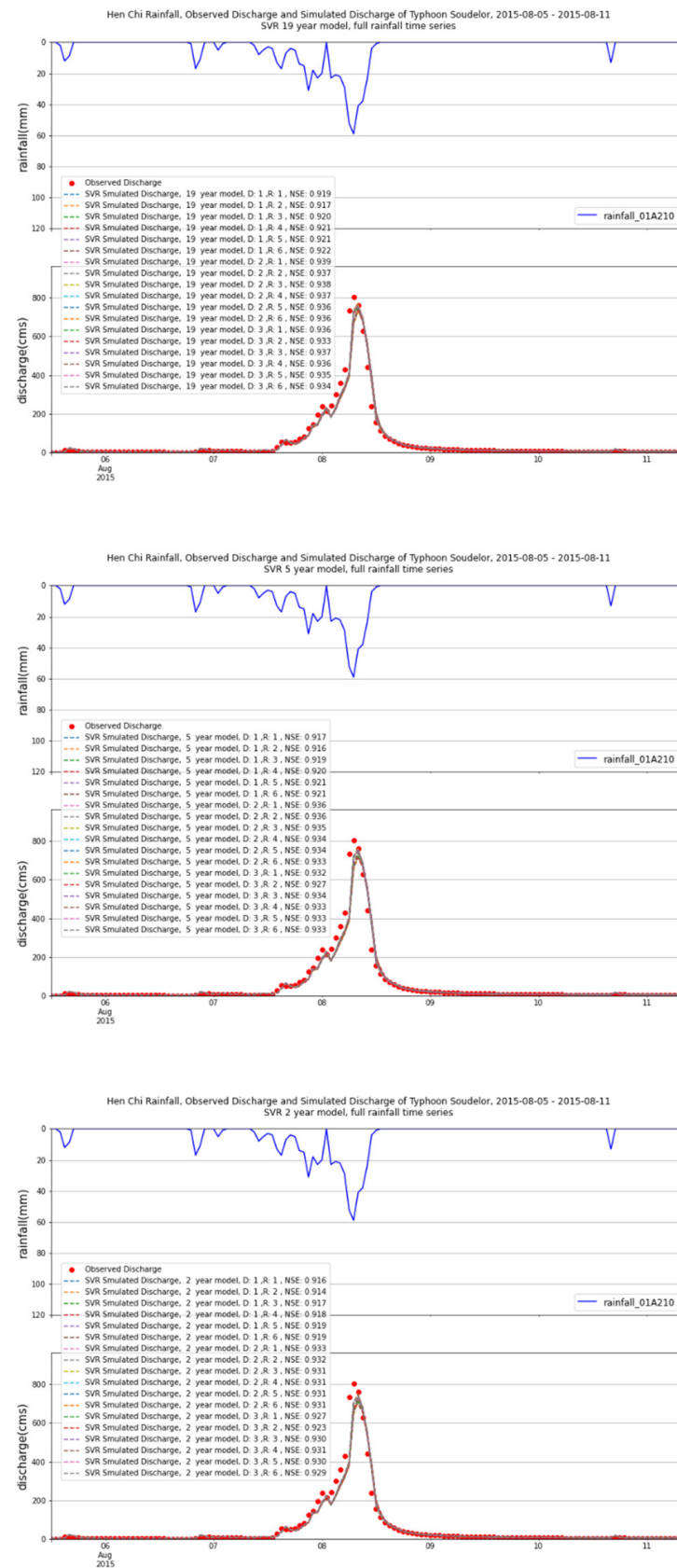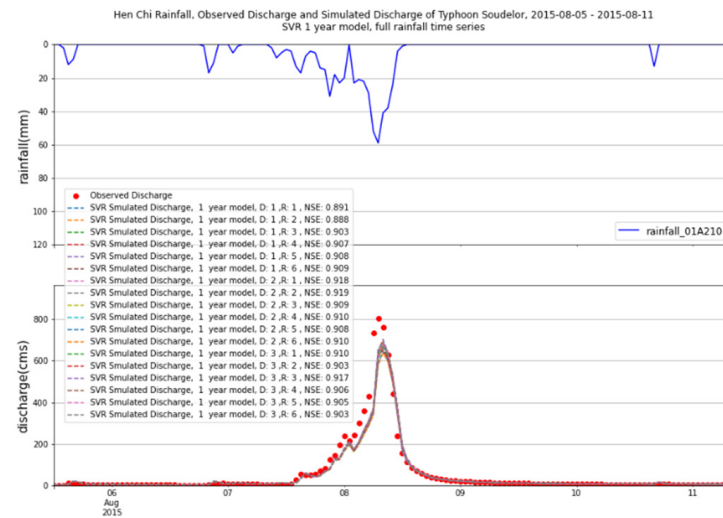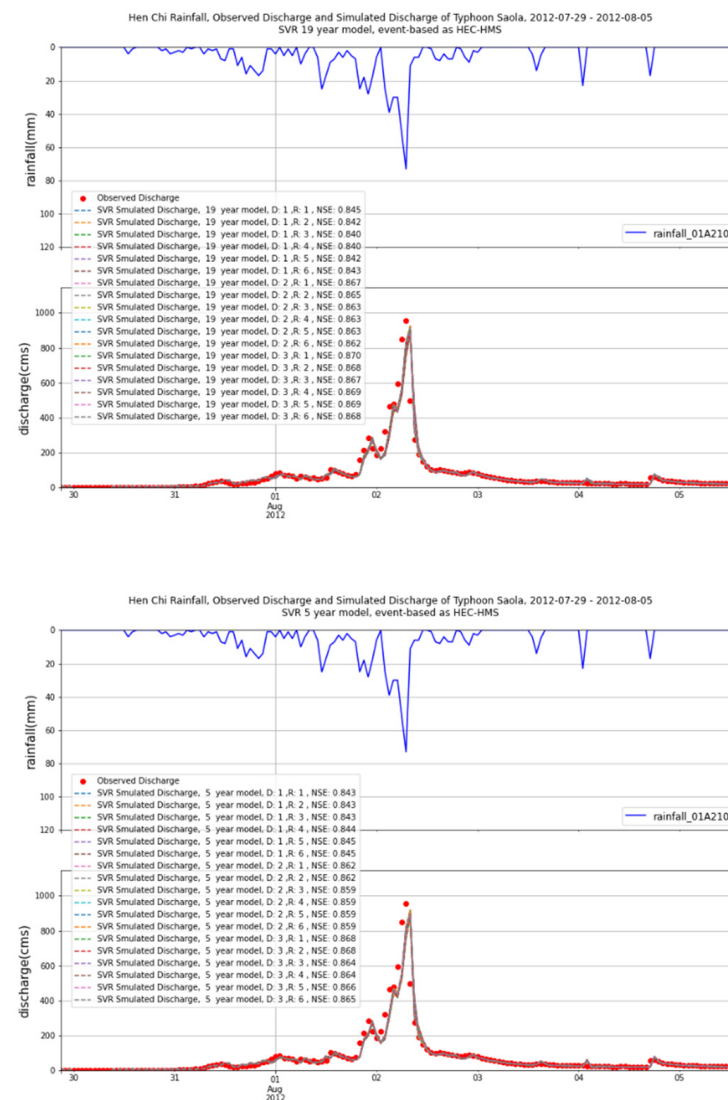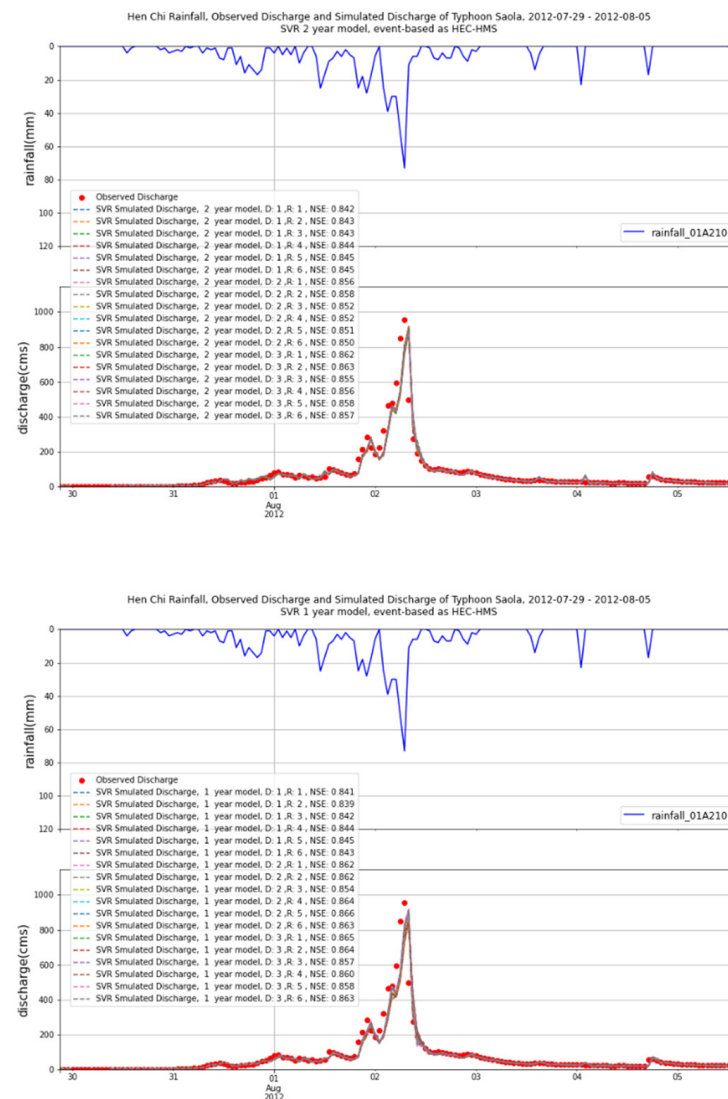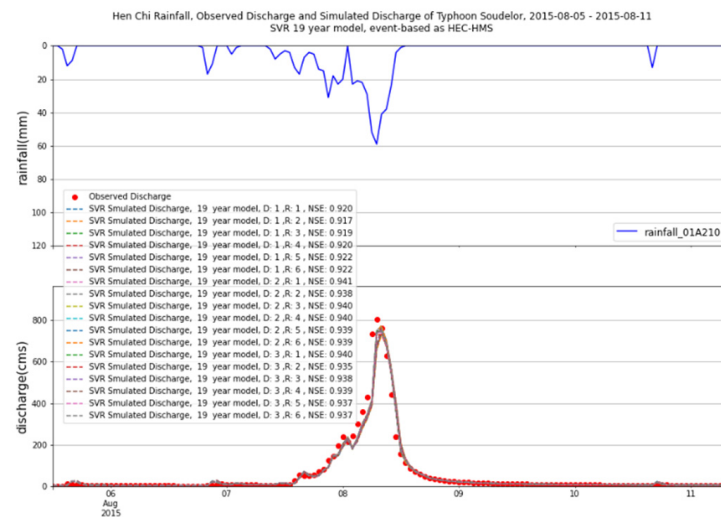
Figure 7. *Cont.*

Figure 7. The testing results derived from the Type 1 SVR model using different features selection for Typhoon Soudelor. D 1 to 3 represents discharge features of the previous 1 to 3 h, while R 1 to 6 indicates rainfall features of the previous 1 to 6 h.
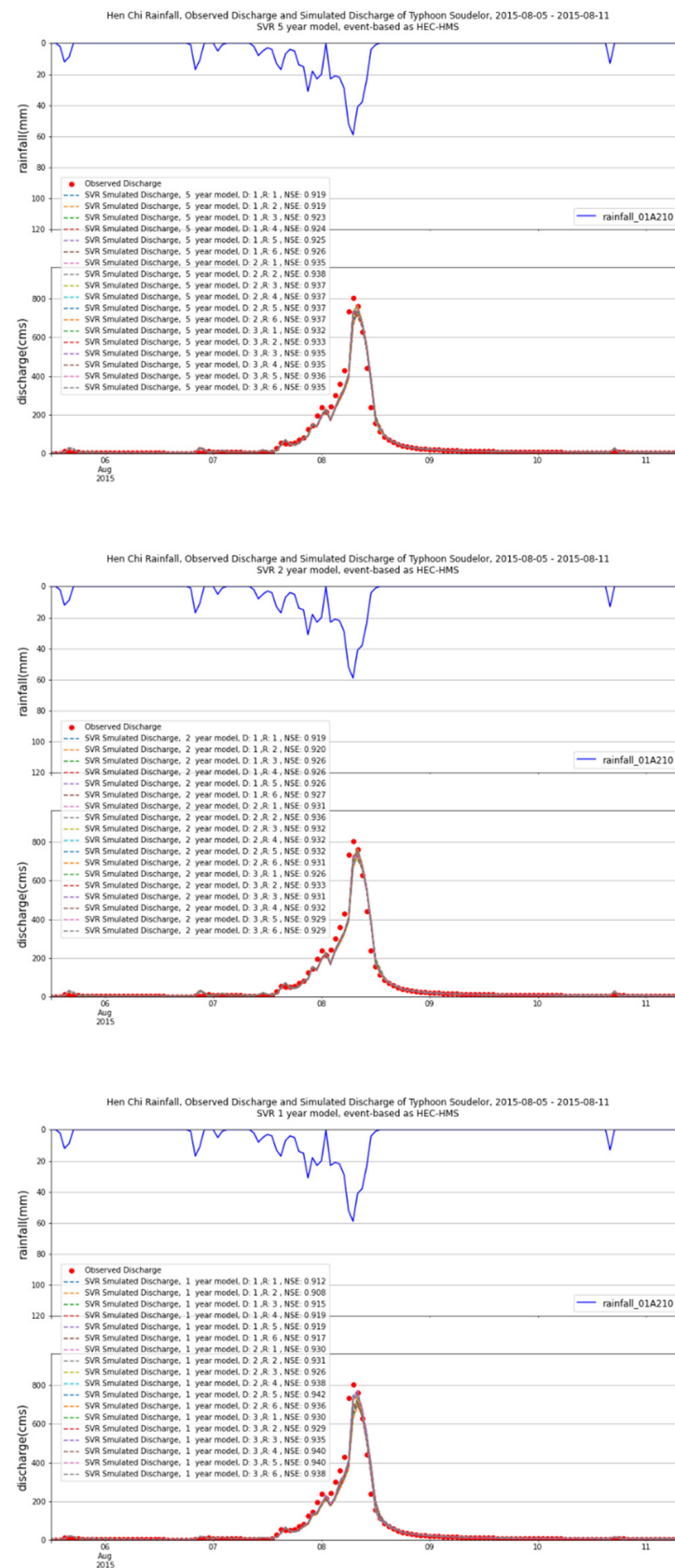

Figure 8. *Cont.*

Figure 8. The testing results derived from the Type 2 SVR model using different features selection for Typhoon Saola. D 1 to 3 represents discharge features of the previous 1 to 3 h, while R 1 to 6 indicates rainfall features of the previous 1 to 6 h.


Figure 9. *Cont.*

Figure 9. The testing results derived from the Type 2 SVR model using different features selection for Typhoon Soudelor. D 1 to 3 represents discharge features of the previous 1 to 3 h, while R 1 to 6 indicates rainfall features of the previous 1 to 6 h.

3.3. Comparison among Model Validation and Test Results

For the convenience of model performance comparison purposes, the model validation and test results are demonstrated in Figures 10 and 11 corresponding to different typhoon events: Saola (2012) and Soudelor (2015). The results showed that the SVR model was far superior to the HEC-HMS within different data time ranges or parameter inference methods. Even if observational data from 1-year or a typhoon event was used for the SVR model training, the SVR model could still infer the target discharge. Table 7 shows the parameter optimization results of the HEC-HMS of Typhoon Saola and Soudelor. It can be seen that tuning the values of parameters could make the model performance better, even close to the SVR model. Nevertheless, the inference methodology of the parameter value is an issue that needs lots of further effort.
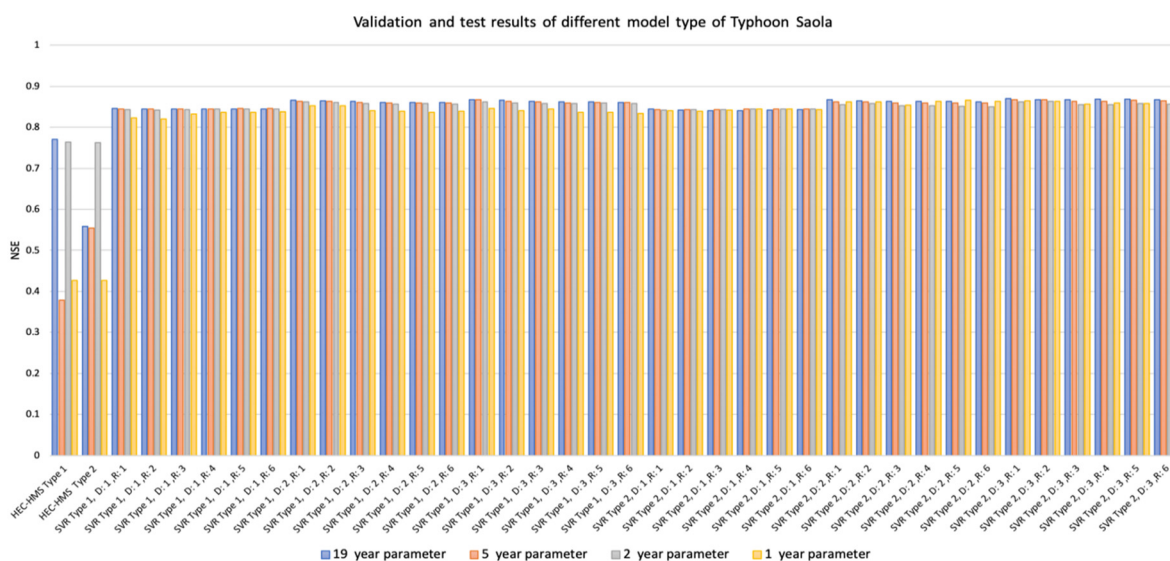
Figure 10. The *NSE* of the SVR and HEC-HMS models validation and test using different approaches for Typhoon Saola.
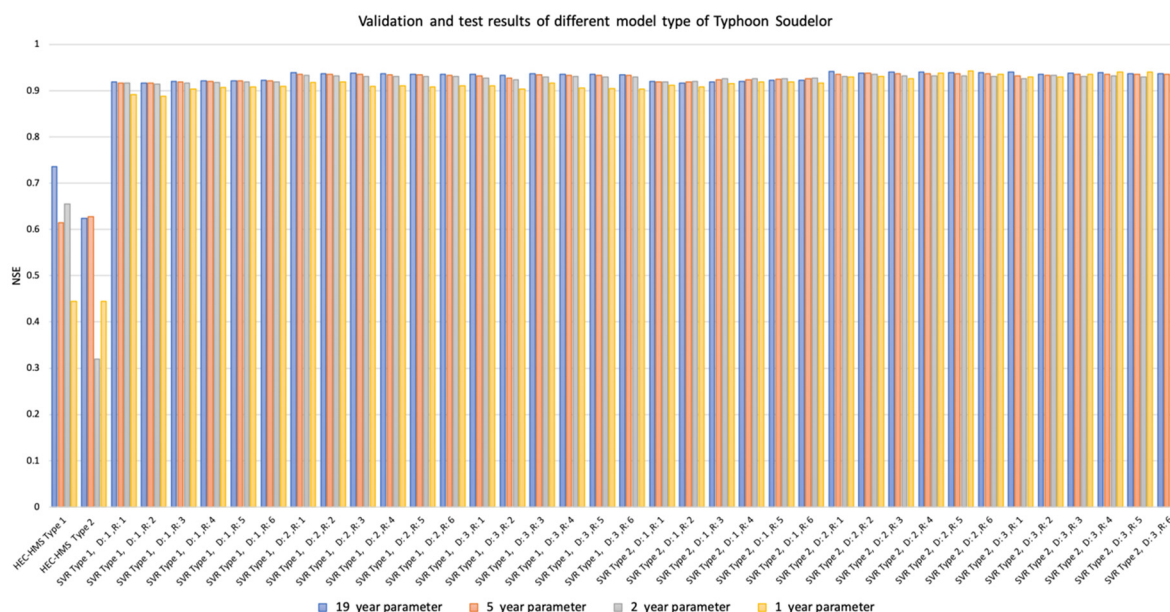
Figure 11. The *NSE* of the SVR and HEC-HMS models validation and test using different approaches for Typhoon Soudelor.

Table 7. Parameter optimization results of the HEC-HMS of the study events.

Typhoon Number	Typhoon Name	Nash–Sutcliffe Coefficient after Optimization
201209	SAOLA	0.856
201513	SOUDELOR	0.932

4. Discussion and Conclusions

The HEC-HMS and SVR, a physically based model and a data-driven hydrologic model were used to identify the adaptability within different lengths of field observation data in the manner of parameters determination (for HEC-HMS) and model training (for SVR). Two types of parameter determination methods were applied for the HEC-HMS model validation process: one by using SVR, with optimized parameter values derived from the typhoon events which occurred within a specific time range, i.e., 19, 5, 2, and 1 year(s), with target and maximum rainfall value, rainfall duration, total rainfall depth as feature values, to acquire the model validation parameter values, named Type 1 HEC-HMS in the study; the other one by manipulating the average optimized parameter values retrieved from the typhoon events which occurred within the same specific time range as Type 1 HEC-HMS, denoted as Type 2 HEC-HMS in the study. Regarding the SVR, two different model training strategies were applied. One was the utilization of the continuous observation data with specific data length, i.e., 19, 5, 2, and 1 year(s), for model training, expressed as Type 1 SVR in the present study. The other was utilizing observational data from the typhoon events used with the HEC-HMS, mentioned previously, for model training and designated as Type 2 SVR in the study. The results showed that the SVR model could estimate an excellent rainfall-runoff relationship even with a shorter period, for instance, only one rainfall event with high-quality time series observation data; however, the HEC-HMS needed many further efforts to achieve similar results. Moreover, different feature value selecting strategies were applied. The conclusions derived from the present study are as follows:

1. The validation results showed that Type 2 HEC-HMS performed better than Type 1 HEC-HMS.
2. The model whose parameter values were derived from multiple typhoon events performed better than the model whose parameter values were derived from only one typhoon event. The model performance was not always proportional to the number of rainfall events for the parameter calibration process, even with the excellent performance of the HEC-HMS during the calibration phase, which might indicate that a global optimization strategy is needed to improve the model validation performance.
3. As for the SVR trained models, Type 2 SVR was slightly better than Type 1 SVR; the rainfall pattern of the validation events being typhoons might be the reason.
4. Furthermore, even within a concise time range of model training, for instance, only one typhoon event, the SVR model could estimate an excellent rainfall-runoff relationship.
5. As for the features selection of the SVR model, when the discharge data of the previous 2-time steps to the target were applied, the model validation results were generally better than the other features selection. The rainfall data features of the previous time step were also proportional to the model validation performance, but not as much as the discharge features were.
6. It could be seen that Type 2 SVR within one typhoon event for model training performed better than Type 1 SVR, which utilized one-year rainfall and discharge data for training. The possible reason might be that the rainfall pattern, which was a typhoon, of the validation event was the same as in Type 2 SVR model training. Other rainfall patterns for model training might give different results. This indicates that data quality is essential for SVR model training.
7. The quality of observation data is essential to using the HEC-HMS and the SVR model. However, the HEC-HMS would need the extra effort of field data collection to determine the geographically related parameters such as land use and soil type;

additional parameter optimization efforts would also be needed. While SVR is easier to apply if excellent observation data is available with good features selection. The maximum discharge of the validation typhoon events was far more significant than the events used for model calibration. Nevertheless, the SVR model could still give an excellent rainfall-runoff estimation.

Additionally, several future efforts could be noted:

1. In the study, the HEC-HMS model parameters estimation by the SVR model was applied, more data-driven based inference of HEC-HMS model parameters is worth studying.
2. This study does not include kernel function selection and its related parameter determination of the SVR model; it is worthwhile to identify a suitable kernel function and other proper parameters in future studies.
3. Selection criteria of the feature dataset for SVR model training could be discussed more.
4. Observation typhoon data was applied in the study; different rainfall patterns and more training and testing events are necessary to validate the comparison results in future studies.
5. The study area is a small rural basin in Northern Taiwan; a more complex and meteorologically different basin could be the future topic of study.

References

1. Singh, V.P.; Woolhiser, D.A. Mathematical Modeling of Watershed Hydrology. *J. Hydrol. Eng.* **2002**, *7*, 270–292. [CrossRef]
2. Singh, V.P.; Frevert, D.K. *Watershed Models*; CRC Press: Boca Raton, FL, USA, 2010.
3. Rangari, V.A.; Sridhar, V.; Umamahesh, N.V.; Patel, A.K. Rainfall Runoff Modelling of Urban Area Using HEC-HMS: A Case Study of Hyderabad City. In *Advances in Water Resources Engineering and Management*; AlKhaddar, R., Singh, R.K., Dutta, S., Kumari, M., Eds.; Lecture Notes in Civil Engineering; Springer: Singapore, 2020; Volume 39, pp. 113–125. ISBN 9789811381805.
4. HEC-HMS. Available online: https://www.hec.usace.army.mil/software/hec-hms/ (accessed on 2 July 2021).
5. Gunathilake, M.B.; Panditharathne, P.; Gunathilake, A.S.; Warakagoda, N.D. Application of HEC-HMS Model on Event-Based Simulations in the Seethawaka Ganga River, Sri Lanka. *In Sch. J. Appl. Sci. Res.* **2019**, *2*, 32–40.
6. Gyawali, R.; Watkins, D.W. Continuous Hydrologic Modeling of Snow-Affected Watersheds in the Great Lakes Basin Using HEC-HMS. *J. Hydrol. Eng.* **2013**, *18*, 29–39. [CrossRef]
7. Ouédraogo, W.; Raude, J.; Gathenya, J. Continuous Modeling of the Mkurumudzi River Catchment in Kenya Using the HEC-HMS Conceptual Model: Calibration, Validation, Model Performance Evaluation and Sensitivity Analysis. *Hydrology* **2018**, *5*, 44. [CrossRef]
8. Bhuiyan, H.; McNairn, H.; Powers, J.; Merzouki, A. Application of HEC-HMS in a Cold Region Watershed and Use of RADARSAT-2 Soil Moisture in Initializing the Model. *Hydrology* **2017**, *4*, 9. [CrossRef]
9. Mount, N.J.; Maier, H.R.; Toth, E.; Elshorbagy, A.; Solomatine, D.; Chang, F.-J.; Abrahart, R.J. Data-Driven Modelling Approaches for Socio-Hydrology: Opportunities and Challenges within the Panta Rhei Science Plan. *Hydrol. Sci. J.* **2016**, *61*, 1–17. [CrossRef]
10. Chen, W.-B.; Liu, W.-C.; Hsu, M.-H. Comparison of ANN approach with 2D and 3D hydrodynamic models for simulating estuary water stage. *Adv. Eng. Softw.* **2012**, *45*, 69–79. [CrossRef]

11. Chen, W.-B.; Liu, W.-C.; Hsu, M.-H. Predicting typhoon-induced storm surge tide with a two-dimensional hydrodynamic model and artificial neural network model. *Nat. Hazards Earth Syst. Sci.* **2012**, *2*, 3799–3809. [CrossRef]

12. Chen, W.-B.; Liu, W.-C. Artificial neural network modeling of dissolved oxygen in reservoir. *Environ. Monit. Assess.* **2014**, *186*, 1203–1217. [CrossRef]

13. Guo, W.-D.; Chen, W.-B.; Yeh, S.-H.; Chang, C.-H.; Chen, H. Prediction of river stage using multistep-ahead machine learning techniques for a tidal river of Taiwan. *Water* **2021**, *13*, 920. [CrossRef]

14. Solomatine, D.; See, L.M.; Abrahart, R.J. Data-Driven Modelling: Concepts, Approaches and Experiences. In *Practical Hydroinformatics*; Abrahart, R.J., See, L.M., Solomatine, D.P., Eds.; Water Science and Technology Library; Springer: Berlin/Heidelberg, Germany, 2008; Volume 68, pp. 17–30. ISBN 978-3-540-79880-4.

15. Solomatine, D.P.; Ostfeld, A. Data-Driven Modelling: Some Past Experiences and New Approaches. *J. Hydroinf.* **2008**, *10*, 3–22. [CrossRef]

16. Barbero, G.; Moisello, U.; Todeschini, S. Evaluation of the areal reduction factor in an urban area through rainfall records of limited length: A case study. *J. Hydrol. Eng.* **2014**, *19*, 05014016-1-10. [CrossRef]

17. Seo, J.-H.; Lee, Y.H.; Kim, Y.-H. Feature Selection for Very Short-Term Heavy Rainfall Prediction Using Evolutionary Computation. *Adv. Meteorol.* **2014**, *2014*, 1–15. [CrossRef]

18. Rodríguez-Pérez, R.; Vogt, M.; Bajorath, J. Support Vector Machine Classification and Regression Prioritize Different Structural Features for Binary Compound Activity and Potency Value Prediction. *ACS Omega* **2017**, *2*, 6371–6379. [CrossRef] [PubMed]

19. Vapnik, V.; Golowich, S.; Smola, A. Support Vector Method for Function Approximation, Regression Estimation, and Signal Processing. In Proceedings of the Advances in Neural Information Processing Systems 9; Mozer, M., Jordan, M., Petsche, T., Eds.; MIT Press: Cambridge, MA, USA, 1997; pp. 281–287.

20. Zaji, A.H.; Bonakdari, H. Optimum Support Vector Regression for Discharge Coefficient of Modified Side Weirs Prediction. *INAE Lett.* **2017**, *2*, 25–33. [CrossRef]

21. Granata, F.; Gargano, R.; de Marinis, G. Support Vector Regression for Rainfall-Runoff Modeling in Urban Drainage: A Comparison with the EPA's Storm Water Management Model. *Water* **2016**, *8*, 69. [CrossRef]

22. Dibike, Y.B.; Velickov, S.; Solomatine, D. Support Vector Machines: Review and Applications in Civil Engineering. *AI Methods Civil Eng. Appl.* **2000**, *14*, 45–58.

23. Nash, J.E.; Sutcliffe, J.V. River Flow Forecasting through Conceptual Models Part I—A Discussion of Principles. *J. Hydrol.* **1970**, *10*, 282–290. [CrossRef]

24. Cronshey, R. *Urban Hydrology for Small Watersheds*; No. 55. US Department of Agriculture, Soil Conservation Service, Engineering Division: Washington, DC, USA, 1986.

25. Clark, C.O. Storage and the Unit Hydrograph. *Trans. Am. Soc. Civ. Eng.* **1945**, *110*, 1419–1446. [CrossRef]

26. Nagy, E.D.; Torma, P.; Bene, K. Comparing Methods for Computing the Time of Concentration in a Medium-Sized Hungarian Catchment. *Slovak J. Civ. Eng.* **2016**, *24*, 8–14. [CrossRef]

27. Straub, T.D.; Melching, C.S.; Kocher, K.E. *Equations for Estimating Clark Unit-Hydrograph Parameters for Small Rural Watersheds in Illinois*; US Department of the Interior, US Geological Survey: Denver, CO, USA, 2000.

28. Ahmad, M.M.; Ghumman, A.R.; Ahmad, S. Estimation of Clark's Instantaneous Unit Hydrograph Parameters and Development of Direct Surface Runoff Hydrograph. *Water Resour. Manag.* **2009**, *23*, 2417–2435. [CrossRef]

29. Che, D.; Nangare, M.; Mays, L.W. Determination of Clark's Unit Hydrograph Parameters for Watersheds. *J. Hydrol. Eng.* **2014**, *19*, 384–387. [CrossRef]

30. Yoo, C.; Lee, J.; Park, C.; Jun, C. Method for Estimating Concentration Time and Storage Coefficient of the Clark Model Using Rainfall-Runoff Measurements. *J. Hydrol. Eng.* **2014**, *19*, 626–634. [CrossRef]

31. Vijay, P. *Singh Hydrologic Systems: Vol. 1: Rainfall-Runoff Modeling*, 1988th ed.; Prentice Hall: Hoboken, NJ, USA, 1988; ISBN 978-0-13-448051-0.

32. Raghavendra, N.S.; Paresh, C.D. Support Vector Machine Applications in the Field of Hydrology: A Review. *Appl. Soft Comput.* **2014**, *19*, 372–386. [CrossRef]

33. Vapnik, V.N. *The Nature of Statistical Learning Theory*; Springer New York: New York, NY, USA, 2000; ISBN 978-1-4419-3160-3.

34. Chang, C.-C.; Lin, C.-J. LIBSVM: A Library for Support Vector Machines. *ACM Trans. Intell. Syst. Technol.* **2011**, *2*, 1–27. [CrossRef]

35. Zhao, H.; Magoules, F. Feature Selection for Support Vector Regression in the Application of Building Energy Prediction. In Proceedings of the 2011 IEEE 9th International Symposium on Applied Machine Intelligence and Informatics (SAMI), Smolenice, Slovakia, 27–29 January 2011; IEEE: Piscataway, NJ, USA, 2011; pp. 219–223.

36. Callegari, M.; Mazzoli, P.; de Gregorio, L.; Notarnicola, C.; Pasolli, L.; Petitta, M.; Pistocchi, A. Seasonal River Discharge Forecasting Using Support Vector Regression: A Case Study in the Italian Alps. *Water* **2015**, *7*, 2494–2515. [CrossRef]